# Controlling the Chiral Inversion Reaction of the Metallopeptide Ni-Asparagine-Cysteine-Cysteine with Dioxygen

Amanda M. Glass,[†] Mary E. Krause,[‡] Jennifer S. Laurence,*,[‡] and Timothy A. Jackson*,[†]

[†]Department of Chemistry and [‡]Department of Pharmaceutical Chemistry, University of Kansas, Lawrence, Kansas 66045, United States

S *Supporting Information*

ABSTRACT: Synthetically generated metallopeptides have the potential to serve a variety of roles in biotechnology applications, but the use of such systems is often hampered by the inability to control secondary reactions. We have previously reported that the Ni[II] complex of the tripeptide LLL-asparagine-cysteine-cysteine, LLL-Ni[II]-NCC, undergoes metal-facilitated chiral inversion to DLD-Ni[II]-NCC, which increases the observed superoxide scavenging activity. However, the mechanism for this process remained unexplored. Electronic absorption and circular dichroism studies of the chiral inversion reaction of Ni[II]-NCC reveal a unique dependence on dioxygen. Specifically, in the absence of dioxygen, the chiral inversion is not observed, even at elevated pH, whereas the addition of O_2 initiates this reactivity and concomitantly generates superoxide. Scavenging experiments using acetaldehyde are indicative of the formation of carbanion intermediates, demonstrating that inversion takes place by deprotonation of the alpha carbons of Asn1 and Cys3. Together, these data are consistent with the chiral inversion being dependent on the formation of a Ni[III]-NCC intermediate from Ni[II]-NCC and O_2. The data further suggest that the anionic thiolate and amide ligands in Ni[II]-NCC inhibit $C\alpha-H$ deprotonation for the Ni[II] oxidation state, leading to a stable complex in the absence of O_2. Together, these results offer insights into the factors controlling reactivity in synthetic metallopeptides.
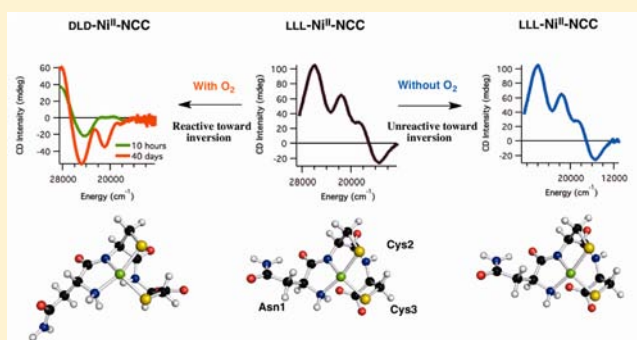
INTRODUCTION

Metal-peptide complexes (metallopeptides) can serve as important biotechnological tools, due in part to their ability to facilitate drug delivery, affect DNA cleavage, and enhance site-specific protein modifications.[1−8] In addition, metallopeptides offer an attractive advantage over their full-length metalloprotein analogues for the mimicking of structure and function, as the small-molecule complexes are often easy to handle and produce in the laboratory, yet can still provide chemical insight into the corresponding biological reactions.[9,10] However, many metallopeptides undergo peptide-modifying reactions that lead to a change in structure and/or chemical properties.[4,11−14] Strict control of the reactivity of these complexes is necessary to achieve the desired chemistry and avoid either deleterious side reactions or inactivation of the complex.

Metal-facilitated peptide modifications include ligand oxidation, spontaneous disulfide bond formation, decarboxylation, hydroxylation, and racemization.[11,15−18] It was recognized in the 1960s that peptide binding to transition metals, such as Co[II], Co[III], Cu[II] and Ni[II], can lead to amino acid racemization under conditions of elevated pH and/or temperature.[18−23] The rates of these racemization reactions show a first-order dependence on OH$^-$ concentration,[24] and carbanion intermediates have been detected using acetaldehyde as a trapping agent.[19] The initiating step in peptide racemization was therefore proposed to be deprotonation of the $C\alpha-H$ group to generate a carbanion intermediate that is subsequently quenched by a proton. Presumably, coordination of the amino or carboxylate group of the peptide to the metal center sufficiently lowers the pK_a of the $C\alpha-H$ group to support deprotonation at elevated pH and/or high temperature. In fact, it has been proposed that for the carboxy-terminal amino acid residue to undergo inversion, the carboxylate must be bound to the metal center.[20]

We previously published the first example of a metal-peptide complex that undergoes chiral inversion at neutral pH and room temperature.[3] The metal-tripeptide complex nickel(II)-asparagine-cysteine-cysteine, ([Ni[II]-NCC]$^{2-}$ or Ni[II]-NCC), undergoes chiral inversion under ambient conditions at pH 7.3 (Figure 1, bottom).[3] The CD spectra of freshly prepared Ni[II]-NCC and the same sample aged 40 days show a complete change in sign in many features (Figure 1, top), indicative of the chiral inversion reaction.[3] At 24 h of aging, an intermediate spectrum is observed (Figure 1, top). On the basis of comparison of the CD spectra of aged Ni[II]-NCC with that of authentic D-containing Ni[II]-NCC compounds, it was concluded
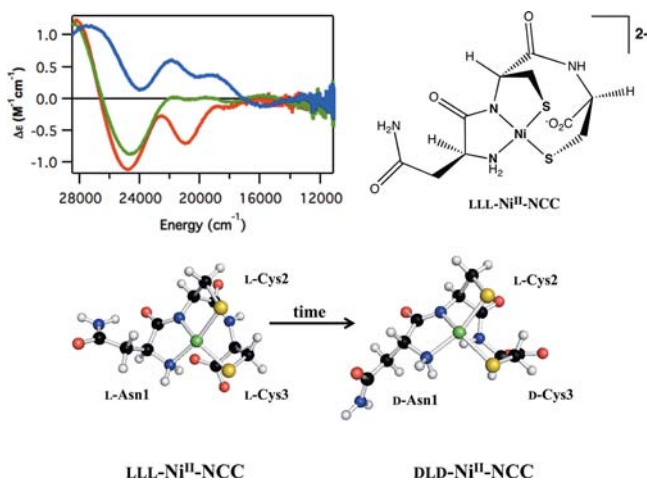
Figure 1. Top left: CD spectra of O$_2$-exposed LLL-Ni^{II}-NCC freshly prepared (blue), aged 10 h (green) and aged 40 days (red). Top right: ChemDraw rendering of LLL-Ni^{II}-NCC. Bottom: Structures of LLL-Ni^{II}-NCC (left) and DLD-Ni^{II}-NCC (right).

that LLL-Ni^{II}-NCC converts completely to DLD-Ni^{II}-NCC. Density functional theory (DFT) calculations suggest the chiral inversion is thermodynamically driven, with an 11 kcal/mol stabilization for DLD-Ni^{II}-NCC relative to the LLL isomer.[3] Preliminary studies that investigated the pH dependence of this process did not support a first-order rate dependence on OH$^-$ concentration, suggesting a novel mechanism for chiral inversion. Indeed, the nickel(II) coordination in Ni^{II}-NCC is distinct from that of other metallopeptides that undergo chiral inversion.[23] Other metallopeptides that undergo racemization feature metal centers coordinated in a mixed 4N/O environment, whereas Ni-NCC employs both nitrogen and sulfur ligands in its square-planar 2N:2S first coordination sphere (Figure 1, bottom).

In addition, Ni^{II}-NCC is both a structural and functional mimic of nickel superoxide dismutase, Ni-SOD, which catalyzes the breakdown of the toxic byproduct of aerobic metabolism, superoxide.[25] The square planar 2N:2S coordination environment in Ni^{II}-NCC is supported by comparison of the Ni^{II}-NCC d-d electronic transition energies with those of native Ni^{II}−SOD, as well as other structural mimics.[9,25−28] Although thiolate ligation is known to tune the reduction potential of the nickel centers in metalloenzymes,[29] it is curious that nature employs sulfur ligation in Ni-SOD. Sulfur ligands are known to be prone to oxidation by O$_2$ and its reduced derivatives, yet during turnover of O$_2^{\bullet-}$ in Ni-SOD, only metal-based oxidation is observed.[30,31] Intriguingly, the extent of chiral inversion in Ni^{II}-NCC is correlated with its superoxide scavenging ability.[3,25]

In this work, we demonstrate that the chiral inversion of LLL-Ni^{II}-NCC to DLD-Ni^{II}-NCC depends critically on dioxygen. Even at elevated pH, the chiral inversion does not occur in the absence of O$_2$. Acetaldehyde trapping experiments suggest the formation of two carbanion intermediates. These data, along with the detection of superoxide when Ni^{II}-NCC is incubated with O$_2$, provide evidence that chiral inversion of LLL-Ni^{II}-NCC proceeds by the formation of a carbanion in a Ni^{III}-NCC intermediate. In the absence of O$_2$, the Ni^{II}-form of NCC is completely inactive toward chiral inversion and stable at least over the course of 10 h. In addition, complementary investigations of DLD-Ni^{II}-NCC suggest this complex is also

reactive when exposed to O$_2$ and may undergo minor secondary reactions such as racemization. The relevance of these data for the reactivity of metallopeptides is discussed.

■ EXPERIMENTAL SECTION

Preparation of O$_2$-Exposed Samples. LLL-NCC was purchased as a lyophilized powder from GenScript, and stored desiccated at −20 °C when not in use. Authentic D-containing peptides, DLD-NCC, LLD-NCC, and DLL-NCC were purchased from NeoBioSci and were stored the same way. The peptide was reconstituted with 50 mM potassium phosphate buffer, generated from dibasic potassium phosphate. Following dissolution, 1.0 or 1.2 mol equiv of NiSO$_4$·6H$_2$O in deionized water were added, and the solution was inverted to ensure good mixing, just before the sample was inserted into the spectrometer for analysis. Samples were adjusted to the appropriate pH with either HCl or KOH, and all pH values reported reflect the final solutions after addition of NCC and NiSO$_4$. Samples generated for spectroscopic analysis were generated with 1.2 mol equiv of Ni^{II} to ensure maximum complex formation, whereas those that were produced for nitroblue tetrazolium (NBT) and acetaldehyde assays were made with 1.0 mol equiv of Ni^{II} ion. The pH range for studying this complex is restricted to basic conditions because at lower pH the complex is altered and precipitation is observed. In addition, at pH values above 9, experimental reproducibility is poor, presumably because the solution is outside the buffering capacity of potassium phosphate.

Preparation of O$_2$-Free Samples. Peptide was reconstituted in 50 mM potassium phosphate buffer of the designated pH and transferred to a quartz cuvette that was stoppered with a Suba-Seal septum and further sealed with parafilm. NiSO$_4$ prepared in water was placed into a small vial secured with a septum and also sealed with parafilm. Samples were purged with 99.5% Ar that was itself purified by passage through columns of activated BASF catalyst and molecular sieves for 20−30 min to remove O$_2$. A total of 1.2 equivalents of Ar-purged NiSO$_4$ in water were transferred to the NCC solution using a gastight syringe. The septum was sealed with parafilm, the solution slowly agitated for ~2 min to ensure proper mixing, and then the cuvette was placed in the spectrometer for data collection and left for the duration of the experiment. We note that both CD and electronic absorption data were closely monitored to ensure the maximum intensity was within 5% of other data sets. This measurement was used to confirm the concentration of the sample was not altered by solvent evaporation during Ar purging. Moreover, the electronic absorption spectra of O$_2$-free and air-exposed Ni-NCC samples reached the same maximum intensity, further supporting that changes in concentration were negligible when purging with Ar.

Electronic Absorption Spectroscopy. Electronic absorption spectra were collected with either a Cary 50 or Agilent 8453 diode array ultraviolet−visible spectrophotometer. All spectra were collected in one cm path length quartz cuvettes with samples at room temperature. O$_2$-exposed samples were stirred during data collection using the interfaced Unisoku cryostat to promote efficient mixing. Ar-purged solutions were not stirred, but were inverted gently prior to data collected to promote efficient mixing. Spectra were collected every 0.1 min for the first 60 min and then every minute thereafter for a minimum of 167 min. To monitor formation of Ni^{II}-NCC for O$_2$-exposed samples, full-spectra were collected for a total of at least 167 min with a spectrum collected every second for the first hour and then attenuated by 1% for each data collection point following.

Nitroblue Tetrazolium Reduction Assay. The nitroblue tetrazolium (NBT) assay was performed to detect the presence of the superoxide anion (O$_2^{\bullet-}$) during the chiral inversion reaction of Ni-NCC. Conversion of NBT (yellow) to its four-electron reduced form, diformazin (blue), results in an increase in absorption at 530 nm. Ni^{II}-NCC was generated by addition of one molar equivalent of 0.1 M NiSO$_4$ in water to 3 mM NCC in pH 7.3 potassium phosphate buffer. The Ni^{II}-NCC mixture was briefly mixed to ensure homogeneity and then the appropriate volume of 12 mM NBT (Alfa Aesar) in pH 7.3 potassium phosphate buffer was added rapidly, to determine the effect

10056

dx.doi.org/10.1021/ic301717q | *Inorg. Chem.* 2012, 51, 10055−10063

of aging Ni^{II}-NCC on the oxidation of NBT to diformazin. Final concentrations of Ni^{II}-NCC and NBT were 0.75 mM and 0.15 mM, respectively. Absorption spectra were collected to monitor the formation of diformazin over the course of 1 h.

Carbanion Trapping with Acetaldehyde. To determine if a carbanion is an intermediate en route to chiral inversion in Ni-NCC, the aging complex was treated with acetaldehyde (ACS Reagent grade, $\geq$ 99.5%, Sigma-Aldrich), and the reaction was monitored via electrospray ionization mass spectrometry (ESI-MS) on an LCT Premier (Waters Corporation) instrument operated in positive ion mode. It has been established that aldehydes can react with carbanion intermediates in solution, resulting in the formation of a product with an increased mass equivalent to that of the deprotonated aldehyde.[22,32] For example, an increase of 43 m/z (the molecular mass of CH_3CHO is 44 Da) indicates the quenching of a single carbanion unit using acetaldehyde. Therefore, we monitored the reaction of acetaldehyde with aging Ni^{II}-NCC via ESI-MS and looked for the formation of a new major ion peak corresponding to an increased mass, indicating quenching of the carbanion and addition of the aldehyde to the ligand. Ni^{II}-NCC was treated with excess (>30 equiv) acetaldehyde, and the reaction was allowed to incubate for at least 24 h at room temperature.

Circular Dichroism (CD) Spectroscopy. CD spectra were collected on a Jasco J-815 spectropolarimeter, using samples generated in quartz cuvettes. Spectra were scanned between 300 and 900 nm (33 333 and 11 111 cm^{-1}) unless otherwise noted. Instrumental parameters included 0.5 s response, 0.2 nm data pitch, 500 nm/min scan rate, and 5 nm bandwidth. Spectra were collected every 10 min for a total of 600 min (61 total spectra collected) unless otherwise noted.

Electron Paramagnetic Resonance (EPR) Spectroscopy. X-band (9 GHz) EPR spectra were collected on a Bruker EMXplus spectrometer, fitted with an Oxford ESR900 continuous-flow liquid helium cryostat and an Oxford ITC503 temperature system to monitor and regulate temperatures. Data were collected at 123 K with liquid nitrogen as the cryogen. LLL-Ni^{II}-NCC samples were generated as described above in pH 7.3, 50 mM potassium phosphate buffer with 1.2 equivalents of $NiSO_4$ added at $t = 0$. Samples were then allowed to age for a designated time. To each sample, a 10% by volume saturated sucrose solution was added as a glassing agent to enhance spectral features. Once prepared, samples were flash frozen in liquid nitrogen and stored at 77 K until data collection. The reproducibility of these experiments was verified by running them in duplicate.

O_2 Addition to O_2-Free Prepared Ni-NCC. Solutions of O_2-free Ni-NCC were generated as described previously. The Ni^{II}-NCC sample was incubated O_2-free for 300 min, and monitored by CD spectroscopy, to ensure maximum Ni^{II}-NCC complex formation. O_2 was added to the sample via bubbling for 1 min. Prior to its addition, the O_2 was stored in a balloon, over a column of DriRite. CD spectra were collected every 10 min for the first 300 min and then 600 min following O_2 addition.

■ RESULTS AND ANALYSIS

**Formation of LLL-Ni^{II}-NCC under O_2-Free Conditions.** Electronic absorption data following the formation of 0.75 mM LLL-Ni^{II}-NCC from free peptide and $NiSO_4$ under O_2-free conditions show a rise in intensity in the visible and UV regions over time (Figure 2). The red spectrum was collected approximately two minutes after metal was added to NCC in O_2-free solutions and represents the earliest accumulated data point for complex formation. The absorption intensity at 21 550 cm^{-1} shows a rapid rise within the first minute of data collection and levels after 150 min (Figure 2, inset). Attempts to model the kinetics of formation of LLL-Ni^{II}-NCC from $NiSO_4$ and LLL-NCC to first-order or second-order rate equations were unsuccessful, which is not surprising given that complex formation likely involves one or more intermediate(s). We had previously reported a drop in absorption intensity as LLL-Ni^{II}-NCC ages under an air atmosphere, which is associated
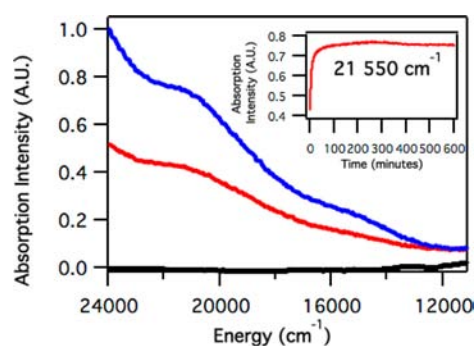
Figure 2. Electronic absorption spectra showing the formation of 0.75 mM LLL-Ni^{II}-NCC under O_2-free conditions in pH 7.3, 50 mM potassium phosphate buffer. The spectra include LLL-NCC without metal (black), Ni-NCC shortly following addition of $NiSO_4$ to LLL-NCC (red), and LLL-Ni^{II}-NCC incubated for 10 h (blue). Inset: absorption intensity at 21 550 cm^{-1} as a function of time.

with the chiral inversion reaction.[3] No drop in absorption intensity is observed under these O_2-free conditions. Moreover, the extinction coefficient for O_2-free LLL-Ni^{II}-NCC is $\varepsilon_{21\,550} = 1\,000$ M^{-1} cm^{-1}, which is substantially greater than that previously reported for O_2-exposed LLL-Ni^{II}-NCC ($\varepsilon_{21\,550} = 300$).

Formation of LLL-Ni^{II}-NCC in the Presence of O_2. Upon addition of $NiSO_4$ to NCC under an air atmosphere, the electronic absorption intensity rises rapidly to 0.75 AU within 10 min (Figure 3). Using the extinction coefficient determined
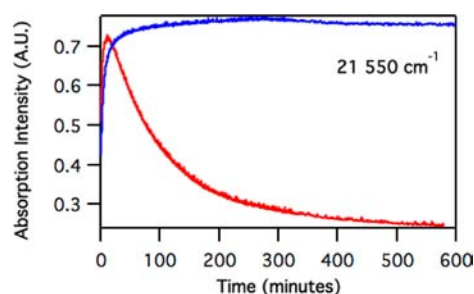
Figure 3. Single-energy (21 550 cm^{-1}) time profile of electronic absorption spectra of 0.75 mM LLL-Ni^{II}-NCC prepared O_2-free (blue) and O_2-exposed (red) in pH 7.3 potassium phosphate buffer.

above, this indicates formation of LLL-Ni^{II}-NCC in ~96% yield. After 10 min of aging, the absorption intensity at this wavelength drops, eventually leveling to 0.25 AU by ~500 min (Figure 3). Assuming the chiral inversion of LLL-Ni^{II}-NCC is responsible for the drop in absorption intensity in the O_2-exposed sample, the inversion reaction proceeds rapidly following formation of LLL-Ni^{II}-NCC specifically in the presence of O_2.

Chiral Inversion Reaction of LLL-Ni^{II}-NCC Does Not Occur in the Absence of O_2. CD spectra of LLL-Ni^{II}-NCC aged for 600 min under argon and air atmospheres are shown in Figure 4. Spectra taken at maximum formation ($t = 10$ min for O_2-exposed samples, $t = 150$ min for O_2-free samples) are very similar but not identical. Both feature four prominent CD signals at 15 500 (−), 19 200 (+), 23 800 (+), and 26 000 (+) cm^{-1}. On the basis of a previously performed deconvolution of electronic absorption and CD spectra, these CD transitions arise from four d-d bands expected for a Ni^{II} ion in a square planar geometry with 2N:2S ligand environment and three S−
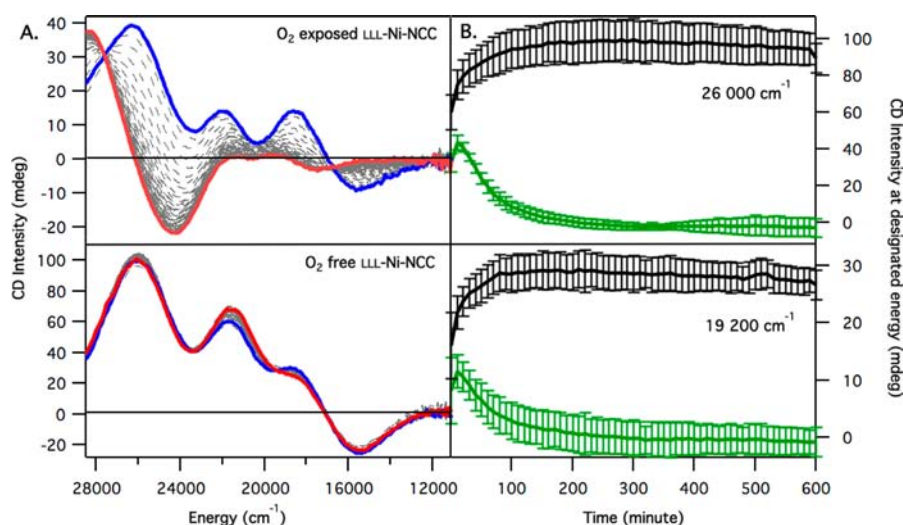
Figure 4. (A) CD spectra of 0.75 mM LLL-Ni^{II}-NCC in pH 7.3 potassium phosphate buffer generated and aged under atmospheres of air (top) and Ar (bottom). Blue spectra were obtained at the time the absorption spectra were at maximum intensity, indicating maximum LLL-Ni^{II}-NCC complex formation (t = 10 min for O$_2$-exposed and t = 150 min for O$_2$-free LLL-Ni^{II}-NCC), red spectra were collected at t = 590 min, and intermediate spectra obtained every 10 min between these two times are represented as gray dashed traces. (B) CD signal at single energies for 0.75 mM LLL-Ni^{II}-NCC incubated O$_2$-free (black) and O$_2$-exposed (green) in pH 7.3 potassium phosphate buffer. Error bars represent ± one standard deviation from an average of three trials.

Ni charge transfer (CT) transitions.[25,33] Starting at t = 0 s, some increase in band intensity is initially observed, especially at 16 300, 19 200, 22 200, and 26 000 cm^{-1}, in both O$_2$-free and O$_2$-exposed LLL-Ni^{II}-NCC, indicating complex formation (Figure 4B). Each band has a slightly different rate of change in formation (data not shown), likely because LLL-Ni^{II}-NCC formation from LLL-NCC and NiSO$_4$ is not a two-state process and involves one or more intermediate(s).

Consistent with our previous report, the time-progression CD spectra of O$_2$-exposed LLL-Ni^{II}-NCC demonstrate distinct sign changes without significant band shifting, indicating chiral inversion of LLL-Ni^{II}-NCC.[3] Major changes occur within the first 10 h, where the absolute intensities of the bands at 16 000 and 23 000 cm^{-1} decrease, and negative bands form at ~17 000 and 24 000 cm^{-1}. This CD spectrum does not look like that previously reported for DLD-Ni^{II}-NCC, but instead resembles that of LLL-Ni^{II}-NCC after 24 h of aging (Figure 1, top).[3] Therefore, this 10-h aged species represents either an intermediate, or a mixture of intermediate species, formed en route to DLD-Ni^{II}-NCC.

In contrast, the CD spectra collected for LLL-Ni^{II}-NCC prepared under an argon atmosphere offer no evidence of chiral inversion. The O$_2$-free sample does demonstrate a change in CD signal within the 600-min time frame; however, these changes occur within the first 150 min and lead solely to an increase in absolute ellipticity (Figure 4B and Supporting Information, Figure S1); that is, no change in sign of any CD features is observed. For O$_2$-free LLL-Ni^{II}-NCC, the individual time traces level after 150 min (Figure 4B), consistent with the time scale for formation of LLL-Ni^{II}-NCC from 1:1 molar ratio of NiSO$_4$ and NCC, as established by the electronic absorption data described above. The intensities of the CD features for O$_2$-free LLL-Ni^{II}-NCC are approximately twice those of O$_2$-exposed LLL-Ni^{II}-NCC, suggesting that the CD spectrum of O$_2$-exposed LLL-Ni^{II}-NCC collected at t = 10 min has contributions from multiple species. The CD spectrum for LLL-Ni^{II}-NCC prepared and aged under an Ar atmosphere therefore represents the authentic CD spectrum of LLL-Ni^{II}-NCC.

**Addition of O$_2$ to LLL-Ni^{II}-NCC Prepared under an Ar Induces the Chiral Inversion Reaction.** Dioxygen gas was added by a syringe to a sample of LLL-Ni^{II}-NCC that was prepared and incubated for 300 min under an Ar atmosphere to allow for maximum LLL-Ni^{II}-NCC formation. The CD spectrum of LLL-Ni^{II}-NCC prepared under an Ar atmosphere, then exposed to O$_2$ (Figure 5), evolves in the same way as the O$_2$-exposed sample (cf. Figures 5 and 4A, top). Thus, chiral inversion of LLL-Ni^{II}-NCC complex is critically dependent on O$_2$.
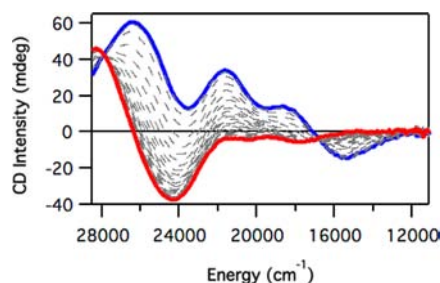
Figure 5. CD spectra of 0.75 mM LLL-Ni^{II}-NCC generated and incubated 300 min under an Ar atmosphere to achieve maximum formation of LLL-Ni^{II}-NCC, then treated with O$_2$. The blue spectrum was collected at t = 300 min to allow for maximum complex formation, and then the sample was injected with O$_2$. The red spectrum was collected after 800 total minutes of incubation (600 min of O$_2$ exposure). Intermediate spectra obtained every 10 min between these two times are represented as gray dashed traces.

Superoxide Is Formed by LLL-Ni^{II}-NCC under an Atmosphere of Air. The nitro blue tetrazolium (NBT) assay was employed to determine if the chiral inversion reaction of LLL-Ni^{II}-NCC involves reduction of O$_2$ to superoxide by the Ni^{II} center. The assay detects formation of O$_2^{\bullet-}$, which oxidizes NBT to its four-electron oxidized species, diformazin (λ_{max} = 530 nm).[34] Solutions containing the Ni-NCC complex and NBT absorbed more strongly at 530 nm than those with NBT
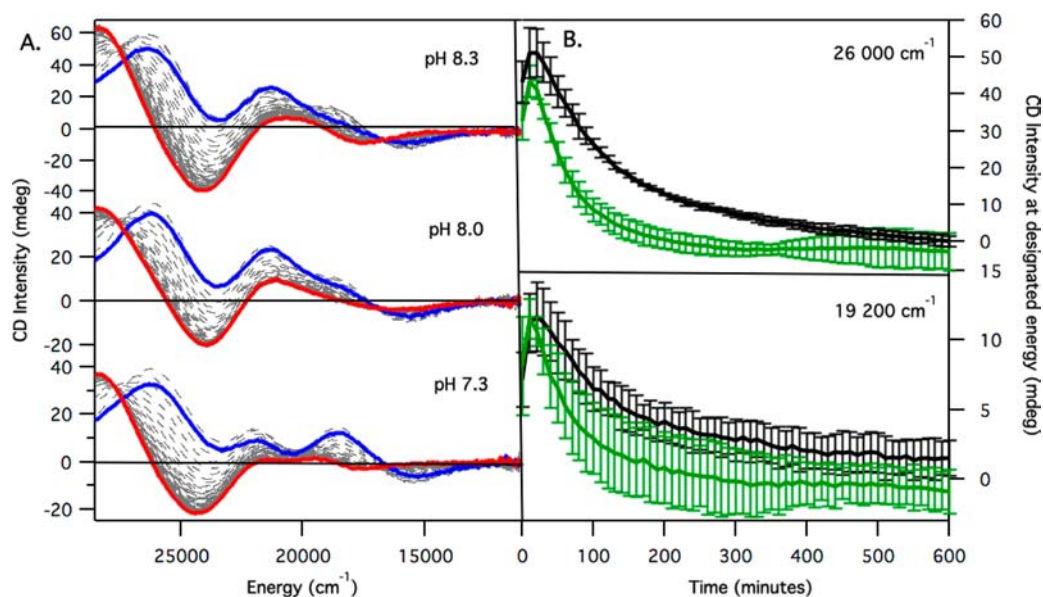
Figure 6. (A) CD spectra of LLL-Ni^{II}-NCC in potassium phosphate buffer at pH 7.3 (bottom), pH 8.0 (middle), and pH 8.3 (top). Blue spectra were collected ~15 s after mixing, red spectra were acquired after 600 min of incubation, and intermediate spectra obtained every 10 min between the two time points are represented as gray dashed traces. (B) CD signal (mdeg) at designated single energies for pH 7.3 (green) and pH 8.3 (black) potassium phosphate solutions. Error bars represent ± one standard deviation from an average of three trials.

alone, Ni-NCC alone, or NBT with only Ni^{II} or NCC, indicating generation of superoxide by Ni^{II}-NCC. In addition, monitoring the absorption at 530 nm over the course of an hour showed an increase in diformazin production, suggesting that superoxide forms as LLL-Ni^{II}-NCC undergoes chiral inversion. Specifically, for O$_2$-exposed Ni^{II}-NCC in the presence of NBT over the course of 30 min, (t = 10 min to t = 40 min) a $\Delta AU_{530\ nm}$ of 0.12 was observed (Supporting Information, Figure S2).

EPR Spectroscopy Provides Evidence for Formation of Ni^{III} in Aging LLL-Ni-NCC. Perpendicular- and parallel-mode X-band EPR spectra collected for freshly prepared LLL-Ni^{II}-NCC samples at 123 K were completely featureless, consistent with the lack of Ni^{III} ions in these samples. However, data collected from duplicate samples aged under an atmosphere of air approximately 10 min showed weak signals in a perpendicular-mode experiment, with g values consistent with Ni^{III} ($g_\perp$ = 2.20 and $g_\parallel$ = 2.05, Supporting Information, Figure S3). The low intensity of the Ni^{III} EPR signal is attributed to a lack of accumulation of the intermediate, which is consistent with the CD data sets. Corresponding EPR data collected for duplicate samples aged 60 min showed the absence of this signal, indicating the consumption of the Ni^{III} species.

LLL-Ni^{II}-NCC Forms Two Carbanion Intermediates En Route to Chiral Inversion. LLL-Ni^{II}-NCC was incubated with excess acetaldehyde to determine if the chiral inversion reaction generates a carbanion intermediate. Aldehydes are known to quench carbanion intermediates in solution and generate a product with a mass increase equal to that of the deprotonated aldehyde.[22,32,35−37] The reaction can be cleanly monitored using ESI-MS operated in positive ion mode. The spectra of LLL-Ni^{II}-NCC incubated with excess acetaldehyde over the course of a day clearly show both the free peptide (339 m/z) and NCC + 2 acetaldehydes (425 m/z) (Supporting Information, Figure S4). These data indicate that over the course of 24 h, two carbanion intermediates are formed per

molecule of LLL-Ni^{II}-NCC. Therefore, each of the single chiral inversion reactions from LLL-Ni-NCC to DLD-Ni-NCC requires a carbanion intermediate.

Chiral Inversion Reaction of LLL-Ni^{II}-NCC Does Not Show First Order Rate Dependence on Hydroxide Ion Concentration. The chiral inversion of LLL-Ni^{II}-NCC was also followed for several different solution pH values, to determine the pH dependence of this reaction. The CD spectra of LLL-Ni^{II}-NCC aged in phosphate buffer at pH 7.3, pH 8.0, and pH 8.3 under an air atmosphere are shown in Figure 6A. For all three solutions, there is an initial increase in CD intensity, indicating LLL-Ni^{II}-NCC complex formation, followed by a change in sign of some CD signals, demonstrating the chiral inversion. Although the t = 0 spectra are not identical for the three different samples (Figure 6A, blue), they all have the same CD bands at the same energies, but with different intensities. This could be attributed to slightly different rates of formation and/or chiral inversion. The dependence on pH of the rate of chiral inversion is shown in Figure 6B, which compares the change in CD signals with time for samples at pH 7.3 and 8.3. While there is a modest effect on the rate of change of the CD signal with the pH of the solution, a first-order dependence in this pH range is not exhibited. Additional experiments at even more elevated pH (>9.0) were performed, but the reproducibility of these results was poor. We speculate that when the solution pH is well outside the buffering capacity of phosphate, slight changes in the amount of LLL-NCC or Ni^{II} used in the experiment perturb the solution pH more significantly and therefore alter the aging progression profile of the complex. Nonetheless, these data collectively demonstrate there is a minor pH effect on the rate of chiral inversion.

To assess whether inversion can occur at elevated pH in the absence of O$_2$, CD spectra were collected for pH 9.0 LLL-Ni^{II}-NCC prepared and aged under an Ar atmosphere. Under these conditions, the only changes observed in the CD spectra are attributed to complex formation (Supporting Information, Figure S5); there is no evidence for chiral inversion. Thus,

regardless of whether LLL-Ni^{II}-NCC is aged in neutral or basic solution, there is no chiral inversion observed in the absence of O$_2$.

DLD-Ni^{II}-NCC Shows Time-Dependent CD Changes. The changes in the CD spectra of DLD-Ni^{II}-NCC aged under an Ar atmosphere are consistent with complex formation (Figure 7,
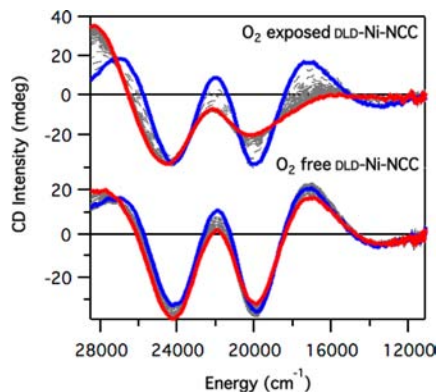
Figure 7. CD spectra of DLD-Ni^{II}-NCC generated in pH 7.3 potassium phosphate buffer and prepared and aged in the absence (bottom) and presence (top) of O$_2$. Spectra were collected at $t = 0$ min (blue), $t = 600$ min (red), and every 10 min in between (gray dashed traces).

bottom). The final spectrum, however, is distinct from that previously reported for DLD-Ni^{II}-NCC.[3] Specifically, in the current spectrum, there is an additional positive feature at 17 000 cm^{-1} not observed previously.[3] Intriguingly, the intensity of this positive feature decreases over time in the O$_2$-exposed sample (Figure 7, top). Thus, CD data collected for DLD-Ni^{II}-NCC in the presence of O$_2$ are consistent with some degree of racemization or secondary reaction. These changes were not detected in the previous study because these modifications happened during the time-course of sample preparation. The 10-h CD spectrum of O$_2$-exposed DLD-Ni^{II}-NCC, however, is essentially identical to that previously reported for aged, O$_2$-exposed LLL-Ni^{II}-NCC.[3] Thus, both LLL-, and DLD-Ni^{II}-NCC proceed to the same end point.

DLL-Ni^{II}-NCC Shows Time-Dependent CD Changes. When prepared under an Ar atmosphere, DLL-Ni^{II}-NCC shows CD changes essentially identical to those of LLL-Ni^{II}-NCC (cf. Figures 8, bottom and 4A, bottom). In both cases, a
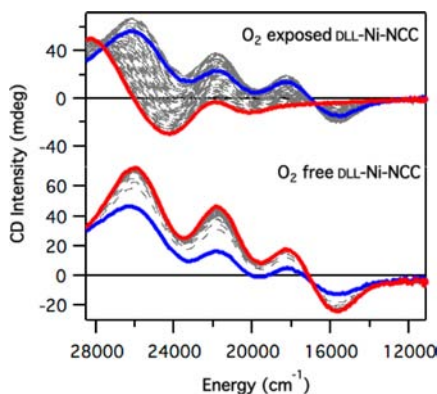
Figure 8. CD spectra of DLL-Ni^{II}-NCC generated in pH 7.3 potassium phosphate buffer and prepared and aged in the absence (bottom) and presence (top) of O$_2$. Spectra were collected at $t = 0$ min (blue), $t = 600$ min (red), and every 10 min in between (dashed gray traces).

negative-signed band at ∼15 500 cm^{-1} and positive features at 19 200, 23 800, and 26 000 cm^{-1} gain intensity. These spectral changes are consistent with full formation of DLL-Ni^{II}-NCC and offer no evidence of chiral inversion. However, when DLL-Ni^{II}-NCC is formed under an air atmosphere, changes in CD signal are observed over the course of 600 min (Figure 9, top),
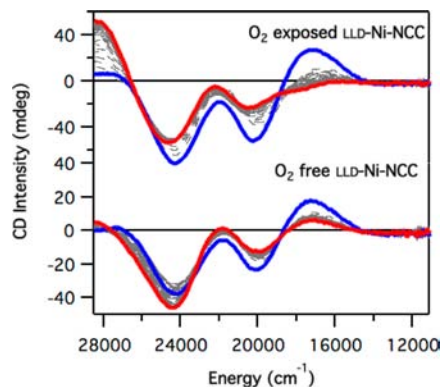
Figure 9. CD spectra of LLD-Ni^{II}-NCC generated in pH 7.3 potassium phosphate buffer and prepared and aged in the absence (bottom) and presence (top) of O$_2$. Spectra were collected at $t = 0$ min (blue), $t = 600$ min (red), and every 10 min in between (dashed gray traces).

consistent with chiral inversion. Specifically, the spectrum collected for DLL-Ni^{II}-NCC after 600 min of aging under air is very similar to that of O$_2$-exposed DLD-Ni^{II}-NCC at 600 min (Figure 7, top).

LLD-Ni^{II}-NCC Undergoes Spectral Changes, Even in the Absence of O$_2$. In the absence of O$_2$, the initial CD spectrum of LLD-Ni^{II}-NCC looks strikingly similar to that of DLD-Ni^{II}-NCC, with a positive band at ∼17 000 cm^{-1} and negative bands at ∼20 000 and 24 500 cm^{-1} (cf. Figures 9, bottom and 7, bottom). When CD data are collected for LLD-Ni^{II}-NCC under an atmosphere of air, the CD features at ∼17 000, 20 000, and 24 000 cm^{-1} lose intensity, with the lowest energy band completely losing CD intensity. Unlike both LLL- and DLD-Ni^{II}-NCC, LLD-Ni^{II}-NCC shows spectral changes even in the absence of O$_2$ (Figure 9, bottom). Given the nature of these spectral changes, this may indicate that the LLD-Ni^{II}-NCC has a propensity for a secondary, nonoxygen-dependent reaction.

■ **DISCUSSION**

Optically active amino acids and peptides are known to undergo racemization in aqueous solution in the absence of metal at temperatures above 100 °C and at pH values above 8 and below 5.[38] Binding of a transition metal to the residues allows the process to occur under milder conditions.[18−24] Metal-bound peptides are able to undergo racemization over the course of hours to days at temperatures between 35 and 40 °C and at a pH above 9. In both cases, the racemization or chiral inversion proceeds by deprotonation of an α carbon. Reprotonation by solvent gives either the D- or L-isomer.[24] Coordination of the amino acid or peptide to a metal center renders the deprotonation event more thermodynamically favorable,[18] leading to racemization or chiral inversion under milder conditions. In most cases where metal-facilitated chiral inversion occurs instead of racemization, steric factors promote the formation of the D-isomer over the L-form.[22,39]

In addition to promoting racemization or inversion, the coordination of peptides to metals is also known to facilitate

peptide degradation and/or oxidation.[22] One example of this is the nickel(II) complex of the tripeptide glycine−glycine-L-histidine, Ni[II]-GGH.[11,13,40] Ni[II]-GGH has been well-studied for its ability to catalyze site-specific oxidation and cleavage of DNA, as well as peptide cross-linking.[17] However, oxidation of Ni[II]-GGH by O$_2$ generates Ni[III]-GGH, which undergoes spontaneous decarboxylation at the C-terminus of the peptide.[13,41] The decarboxylated product undergoes further reactions including hydroxylation and racemization.[13] Additional Ni[III]-mediated reactivity in peptides includes ligand oxidation and disulfide bond formation/peptide cross-linking.[17]

O$_2$-Dependent Chiral Inversion of Ni-NCC. In the absence of O$_2$, LLL-Ni[II]-NCC forms rapidly from NiSO$_4$ and LLL-NCC, and this complex is stable for at least 10 h, showing no evidence of inversion or secondary reactions, even at pH 9.0. This is in contrast to other square planar Ni[II]-peptide complexes that readily undergo base-catalyzed, metal-facilitated racemization at pH ≥ 9 over the course of several hours to days.[19,23,42] We attribute the lack of chiral inversion in LLL-Ni[II]-NCC under anaerobic conditions to the presence of two anionic cysteinate ligands and one anionic amide ligand (Figure 1). Charge donation from these ligands is expected to reduce the Lewis acidity of the Ni[II] center, mitigating the ability of the metal to promote deprotonation of the Cα−H groups. A complementary rationale is that the anionic ligands, along with the deprotonated carboxylate group, give Ni[II]-NCC an overall charge of −2, which would disfavor deprotonation on electrostatic grounds. This same behavior is observed for DLD-Ni[II]-NCC, which is also unchanged for at least 10 h when under an Ar atmosphere.

In the presence of O$_2$, LLL-Ni[II]-NCC shows fairly rapid spectroscopic changes that are consistent with inversion (or racemization) of the NCC peptide. On the basis of trapping experiments with acetaldehyde, two carbanions are formed during the O$_2$-dependent inversion. Studies of the inversion reaction at pH 7.3−8.3 reveal a minor increase in the rate of inversion as the pH is increased. These data are consistent with inversion proceeding by Cα−H deprotonation, but this deprotonation does not occur for LLL-Ni[II]-NCC prepared in the absence of O$_2$. In addition, another step must impact the rate of inversion more significantly than Cα−H deprotonation. The evidence for superoxide formation, as well as the O$_2$ dependence of this reaction, suggest that LLL-Ni[II]-NCC reacts with O$_2$ to form superoxide and LLL-Ni[III]-NCC. We propose the higher oxidation state Ni[III] center promotes Cα−H deprotonation, leading to inversion (or racemization) for LLL-Ni[III]-NCC upon reprotonation. Subsequent reaction of superoxide, or some alternative reductant, with Ni[III]-NCC, would regenerate the Ni[II] complex. Perpendicular-mode X-band EPR spectra collected for frozen aliquots of LLL-Ni[II]-NCC during the aging process showed a very weak feature, the position and line shape of which are consistent with a Ni[III] center ($g_\perp$ = 2.20 and $g_\parallel$ = 2.05), albeit in very low concentration.

The percent conversion of LLL-Ni[II]-NCC to DLD-Ni[II]-NCC can be estimated in a crude manner assuming the CD band at ∼25 000 cm^{-1} for aged LLL-Ni[II]-NCC arises predominantly from DLD-Ni[II]-NCC. Using this approach, it is estimated that the LLL-Ni[II]-NCC complex is 70 and 90% converted to DLD-Ni[II]-NCC after 10 h and 40 days, of aging respectively. We note, however, that these values should be viewed tentatively, as other species, either formed en route to DLD-Ni[II]-NCC or by secondary reactions, could increase or decrease the absolute CD intensity at ∼25 000 cm^{-1}.

Pathway to Chiral Inversion in Ni-NCC. In the presence of oxygen, LLL-Ni[II]-NCC evolves to give a CD spectrum most similar to that of DLD-Ni[II]-NCC. The same behavior is observed for DLL- and LLD-Ni[II]-NCC. Thus, regardless of the initial isomer, all species show a final CD spectrum most similar to that of DLD-Ni[II]-NCC. Under the assumption that the final distribution of Ni[II]-NCC is under thermodynamic, rather than kinetic, control, the directed inversion of Ni[II]-NCC can be rationalized on the basis of DFT-computed energies of models of Ni[II]-NCC (Scheme 1).[3] In the current study, we show that

Scheme 1. Pathway to Chiral Inversion in Ni-NCC, with DFT-Computed Relative Energies of Each Model Shown^a
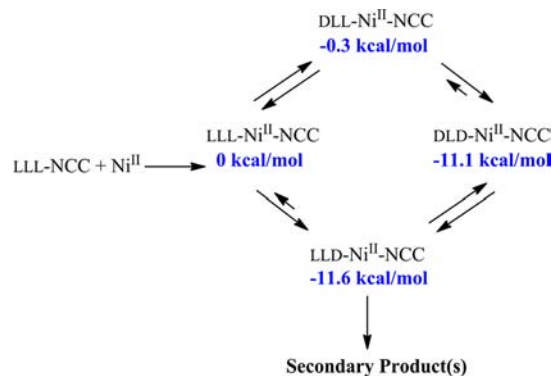
^{a}All energy values are given relative to that of LLL-Ni[II]-NCC, whose energy is defined as 0 kcal/mol.

even DLD-Ni[II]-NCC evolves over time when exposed to O$_2$, although the change is significantly more minor than that observed for LLL-Ni[II]-NCC (cf. Figures 7 and 4), indicating existence of a secondary reaction.

According to our previously reported DFT-computed energies (Scheme 1),[3] the inversion of Asn1 results in very little change in energy, whereas inversion of Cys3 leads to a stabilization of ∼11 kcal/mol. It would be tempting to propose that the spectral changes observed for DLD-Ni[II]-NCC are due to its racemization to a mixture of DLD-Ni[II]-NCC and LLD-Ni[II]-NCC. However, the final CD spectrum cannot be reproduced by addition of the CD spectra of authentic (i.e., O$_2$-free) LLD- and DLD-Ni[II]-NCC in different proportions. In particular, CD spectra of LLD- and DLD-Ni[II]-NCC show a prominent positive band at ∼17 000 cm^{-1}, whereas this band disappears with time in the O$_2$-exposed samples (Figures 7 and 9). Intriguingly, LLD-Ni[II]-NCC shows some spectral changes in the absence of O$_2$, suggesting that this isomer may be reactive even in the Ni[II] oxidation state. The O$_2$-dependent conversion of DLD-Ni[II]-NCC to LLD-Ni[II]-NCC, followed by the formation of some secondary product from the latter complex, could account for the spectral changes observed for O$_2$-exposed DLD-Ni[II]-NCC. Thus, the likely end point in the cycle shown in Scheme 1 is DLD-Ni[II]-NCC in the presence of an intermediate or secondary product that represents a small population of the sample.

The time-progression of the CD and electronic absorption spectra of LLL-Ni[II]-NCC indicate the accumulation of an intermediate after 10 h of incubation with metal. The CD spectrum of this intermediate is identical to that of the 24-h intermediate we described previously,[3] and is nearly featureless below 22 000 cm^{-1} (cf. Figures 1, top and 4A, top). This intermediate is not a singly inverted species, as the CD spectra collected for authentic DLL- and/or LLD-Ni[II]-NCC are quite

different than the corresponding spectrum of the 10-h intermediate. Attempts to reproduce the CD spectrum of the 10-h intermediate via spectral combinations of different proportions of authentic (i.e., O_2-free) LLL-, DLL-, LLD- and DLD-Ni^{II}-NCC were unsuccessful. Specifically, the CD spectra of LLD- and DLD-Ni^{II}-NCC both show a positive band at ~17 000 cm^{-1} whereas those of DLL-Ni^{II}-NCC and LLL-Ni^{II}-NCC have a negative band at ~16 000 cm^{-1}. Therefore, the lower-energy features, although varied in sign, are significantly shifted such that they do not cancel each other out to make the spectrum appropriately featureless below 21 000 cm^{-1}. This suggests that the 10-h-aged intermediate is not simply a mixture of various chiral forms of Ni^{II}-NCC.

Another possible assignment of the 10-h aged intermediate is a Ni^{II}-form of NCC where Cys3 has dissociated from the Ni^{II} center to give a "Cys3-off" configuration. The CD spectra of authentic (i.e., O_2-free) LLD-, and DLD-Ni^{II}-NCC both show a positive band at ~17 000 cm^{-1} (Figures 7 and 9), whereas the CD spectra of LLL-, and DLL-Ni^{II}-NCC show a negative feature near this energy (at ~16 000 cm^{-1}; Figures 4 and 9). Therefore, the band at 17 000 cm^{-1} is directly related to the chiral state of Cys3. Therefore, dissociation of the thiolate of Cys3 from the nickel center could account for the lack of significant CD spectral features below 21 000 cm^{-1}. Considering the structure of LLL-Ni^{II}-NCC (Figure 1), the formation of LLD-Ni^{II}-NCC would likely require dissociation and subsequent religation of Cys3. Thus, it appears reasonable that the CD spectrum of the 10-h aged species has contributions from a species where Cys3 has dissociated from the Ni^{II} center. This "Cys3-off" form of Ni^{II}-NCC could also offer a potential route to the secondary reactions of the complex. Attempts to react the complex with thiol-modifying reagents, however, produced no direct evidence of the "Cys-off" state, suggesting that, if this state does form, it is transient and/or present in very low amounts. For the related enzyme Ni-SOD, removal of one Cys ligand by site-directed mutagenesis led to the lack of any sulfur coordination and the formation of a high-spin ($S = 1$) Ni^{II} protein.[43] We note that ^{1}H NMR experiments on Ni^{II}-NCC have been hampered by the presence of a minor paramagnetic component, which, on the basis of low-temperature, variable-temperature, variable-field magnetic circular dichroism (VTVH MCD) data was assigned to a high-spin Ni^{II} component that represented less than 1% of the sample under the conditions of the VTVH MCD experiment.[25]

Implications of the Controlled Reactivity in Ni^{II}-NCC. The data presented herein underscore the specific and unique reactivity of the Ni^{II}-NCC complexes in the absence of O_2, as well as their complex chemistry when O_2 is available to react with the Ni^{II} center. Superoxide is formed initially during oxygen-dependent chiral inversion, but once inversion occurs, the complex presumably performs antioxidant chemistry, scavenging superoxide. Oxidation to the Ni^{III} form initiates a cascade of reactions that convert the bulk of the sample to DLD-Ni^{II}-NCC. These results have important implications both for controlled reactivity of molecules with biotechnology applications, as well as understanding the diverse chemistry of redox-active, nickel-dependent metalloenzymes. The preferred coordination geometry of a low-spin, thiolate-bound Ni^{II} center is different than that of a Ni^{III} ion (square planar versus distorted octahedral geometry). Thus, the Ni^{III} forms of nickel-peptide complexes must be stabilized in a different fashion than the Ni^{II} centers to prevent undesired secondary or peptide-modifying reactions. This is a significant challenge, as

underscored by the general lack of Ni^{III}-peptide complexes, and the complex reactivity of Ni^{III}-peptides that involves decarboxylation and ligand oxidation reactions.[11–13,16,20,40,41,44–52] For Ni^{II} complexes to be properly used for biotechnology applications, either the Ni^{III} form must be sufficiently stabilized so as to prevent secondary reactions, or the reactivity of the Ni^{II} center with O_2 must be controlled. The Ni-NCC system exhibits far greater stability and reaction specificity than other nickel-peptide systems, making it potentially useful in a variety of applications.

CONCLUSIONS

The research presented here shows that incorporation of Ni^{II} into the LLL-NCC peptide occurs very rapidly and does not undergo chiral inversion in the absence of dioxygen. It further demonstrates that site-specific chiral inversion of LLL-Ni^{II}-NCC to DLD-Ni^{II}-NCC specifically depends on O_2. The chiral inversion reaction produces superoxide and likely proceeds via a Ni^{III} intermediate to generate the DLD-Ni^{II}-NCC product. Because of the specificity of the chiral inversion reaction and stability of the complex, this system is amenable to use as a catalyst in biotechnology and industrial applications.

ASSOCIATED CONTENT

S Supporting Information

Full CD spectra of LLL-Ni^{II}-NCC prepared O_2-free in pH 7.3 and pH 9.0 potassium phosphate, an EPR spectrum of ten-minute aged Ni-NCC, NBT assay single-wavelength time traces, and ESI-MS spectra from the acetaldehyde carbanion trapping reaction. This material is available free of charge via the Internet at http://pubs.acs.org.

AUTHOR INFORMATION

Corresponding Author
*Phone: (785)-864-3968 (T.A.J.), (785)-864-3405 (J.S.L.). Fax: (785)-864-5396 (T.A.J.), (785)-864-5736 (J.S.L.). E-mail: taj@ku.edu (T.A.J.), laurencj@ku.edu (J.S.L.).

Notes
The authors declare no competing financial interest.

REFERENCES

(1) Bal, W.; Chmurny, G. N.; Hilton, B. D.; Sadler, P. J.; Tucker, A. *J. Am. Chem. Soc.* **1996**, *118*, 4727−4728.
(2) Burrows, C. J.; Perez, R. J.; Muller, J. G.; Rokita, S. E. *Pure Appl. Chem.* **1998**, *70*, 275−278.
(3) Krause, M. E.; Glass, A. M.; Jackson, T. A.; Laurence, J. S. *Inorg. Chem.* **2011**, *50*, 2479−2487.
(4) Krężel, A.; Kopera, E.; Protas, A. M.; Poznański, J.; Wysłouch-Cieszyńska, A.; Bal, W. *J. Am. Chem. Soc.* **2010**, *132*, 3355−3366.
(5) Liang, Q.; Eason, P. D.; Long, E. C. *J. Am. Chem. Soc.* **1995**, *117*, 9625−9631.

(6) Lioe, H.; Duan, M.; O'Hair, R. A. J. *Rapid Commun. Mass Spectrom.* **2007**, *21*, 2727−2733.

(7) Shullenberger, D. F.; Eason, P. D.; Long, E. C. *J. Am. Chem. Soc.* **1993**, *115*, 11038−11039.

(8) Splith, K.; Neundorf, I.; Hu, W. N.; N'Dongo, H. W. P.; Vasylyeva, V.; Merz, K.; Schatzschneider, U. *Dalton Trans.* **2010**, *39*, 2536−2545.

(9) Shearer, J.; Long, L. M. *Inorg. Chem.* **2006**, *45*, 2358−2360.

(10) Rabanal, F.; DeGrado, W. F.; Dutton, P. L. *J. Am. Chem. Soc.* **1996**, *118*, 473−474.

(11) Bal, W.; Djuran, M. I.; Margerum, D. W.; Gray, E. T.; Mazid, M. A.; Tom, R. T.; Nieboer, E.; Sadler, P. J. *J. Chem. Soc., Chem. Commun.* **1994**, 1889−1890.

(12) Bossu, F. P.; Paniago, E. B.; Margerum, D. W.; Kirksey, S. T.; Kurtz, J. L. *Inorg. Chem.* **1978**, *17*, 1034−1042.

(13) Green, B. J.; Tesfai, T. M.; Margerum, D. W. *Dalton Trans.* **2004**, 3508−3514.

(14) Kozlowski, H.; Bal, W.; Dyba, M.; Kowalik-Jankowska, T. *Coord. Chem. Rev.* **1999**, *184*, 319−346.

(15) Gale, E. M.; Narendrapurapu, B. S.; Simmonett, A. C.; Schaefer, H. F.; Harrop, T. C. *Inorg. Chem.* **2010**, *49*, 7080−7096.

(16) Haas, K.; Dialer, H.; Piotrowski, H.; Schapp, J.; Beck, W. *Angew. Chem., Int. Ed.* **2002**, *41*, 1879−1881.

(17) Ross, S. A.; Burrows, C. J. *Inorg. Chem.* **1998**, *37*, 5358−5363.

(18) Williams, D. H.; Busch, D. H. *J. Am. Chem. Soc.* **1965**, *87*, 4644−4645.

(19) Buckingham, D. A.; Marzilli, L. G.; Sargeson, A. M. *J. Am. Chem. Soc.* **1967**, *89*, 5133−5138.

(20) Fujioka, M.; Nakao, Y.; Nakahara, A. *Bull. Chem. Soc. Jpn.* **1976**, *49*, 477−479.

(21) Gillard, R. D.; Phipps, D. A. *J. Chem. Soc., Chem. Commun.* **1970**, 800−801.

(22) Pasini, A.; Casella, L. *J. Inorg. Nucl. Chem.* **1974**, *36*, 2133−2144.

(23) Smith, G. G.; Khatib, A.; Reddy, G. S. *J. Am. Chem. Soc.* **1983**, *105*, 293−295.

(24) Stadtherr, L. G.; Angelici, R. J. *Inorg. Chem.* **1975**, *14*, 925−930.

(25) Krause, M. E.; Glass, A. M.; Jackson, T. A.; Laurence, J. S. *Inorg. Chem.* **2010**, *49*, 362−364.

(26) Barondeau, D. P.; Kassmann, C. J.; Bruns, C. K.; Tainer, J. A.; Getzoff, E. D. *Biochemistry* **2004**, *43*, 8038−8047.

(27) Bryngelson, P. A.; Arobo, S. E.; Pinkham, J. L.; Cabelli, D. E.; Maroney, M. J. *J. Am. Chem. Soc.* **2003**, *126*, 460−461.

(28) Shearer, J.; Neupane, K. P.; Callan, P. E. *Inorg. Chem.* **2009**, *48*, 10560−10571.

(29) Kruger, H. J.; Peng, G.; Holm, R. H. *Inorg. Chem.* **1991**, *30*, 734−742.

(30) Grapperhaus, C. A.; Darensbourg, M. Y. *Acc. Chem. Res.* **1998**, *31*, 451−459.

(31) Mirza, S. A.; Pressler, M. A.; Kumar, M.; Day, R. O.; Maroney, M. J. *Inorg. Chem.* **1993**, *32*, 977−987.

(32) Berndt, D. C. *J. Org. Chem.* **1970**, *35*, 1129−1131.

(33) Fiedler, A. T.; Bryngelson, P. A.; Maroney, M. J.; Brunold, T. C. *J. Am. Chem. Soc.* **2005**, *127*, 5449−5462.

(34) Auclair, C.; Voisin, E. *CRC Handbook of Methods for Oxygen Radical Research*; CRC Press: Boca Raton, FL, 1985.

(35) Belokon, Y. N.; Bulychev, A. G.; Vitt, S. V.; Struchkov, Y. T.; Batsanov, A. S.; Timofeeva, T. V.; Tsyryapkin, V. A.; Ryzhov, M. G.; Lysova, L. A.; Bakhmutov, V. I.; Belikov, V. M. *J. Am. Chem. Soc.* **1985**, *107*, 4252−4259.

(36) Casella, L.; Pasini, A.; Ugo, R.; Visca, M. *J. Chem. Soc., Dalton Trans.* **1980**, 1655−1663.

(37) Teo, S. B.; Teoh, S. G. *Inorg. Chim. Acta Lett.* **1980**, *44*, L269−L270.

(38) Bada, J. L. *J. Am. Chem. Soc.* **1972**, *94*, 1371−1373.

(39) Job, R.; Bruice, T. C. *J. Chem. Soc., Chem. Commun.* **1973**, 332−333.

(40) Green, B. J.; Tesfai, T. M.; Xie, Y.; Margerum, D. W. *Inorg. Chem.* **2004**, *43*, 1463−1471.

(41) Tesfai, T. M.; Green, B. J.; Margerum, D. W. *Inorg. Chem.* **2004**, *43*, 6726−6733.

(42) Keyes, W. E.; Caputo, R. E.; Willett, R. D.; Legg, J. I. *J. Am. Chem. Soc.* **1976**, *98*, 6939−6945.

(43) Johnson, O. E.; Ryan, K. C.; Maroney, M. J.; Brunold, T. C. *J. Biol. Inorg. Chem.* **2010**, *15*, 777−793.

(44) Subak, E. J.; Loyola, V. M.; Margerum, D. W. *Inorg. Chem.* **1985**, *24*, 4350−4356.

(45) Bossu, F. P.; Margerum, D. W. *J. Am. Chem. Soc.* **1976**, *98*, 4003−4004.

(46) Farmer, P. J.; Solouki, T.; Mills, D. K.; Soma, T.; Russell, D. H.; Reibenspies, J. H.; Darensbourg, M. Y. *J. Am. Chem. Soc.* **1992**, *114*, 4601−4605.

(47) Gale, E. M.; Cowart, D. M.; Scott, R. A.; Harrop, T. C. *Inorg. Chem.* **2011**, *50*, 10460−10471.

(48) Kirksey, S. T.; Neubecker, T. A.; Margerum, D. W. *J. Am. Chem. Soc.* **1979**, *101*, 1631−1633.

(49) Lappin, A. G.; Murray, C. K.; Margerum, D. W. *Inorg. Chem.* **1978**, *17*, 1630−1634.

(50) Murray, C. K.; Margerum, D. W. *Inorg. Chem.* **1983**, *22*, 463−469.

(51) Owens, G. D.; Phillips, D. A.; Czarnecki, J. J.; Raycheba, J. M. T.; Margerum, D. W. *Inorg. Chem.* **1984**, *23*, 1345−1353.

(52) Paniago, E. B.; Weatherburn, D. C.; Margerum, D. W. *J. Chem. Soc., Chem. Commun.* **1971**, 1427−1428.